Intermittency in the scrape-off layer of the National Spherical Torus Experiment during H-mode confinement

R. J. Maqueda,* D. P. Stotler, S. J. Zweben, and the NSTX team

Princeton Plasma Physics Laboratory, Princeton, NJ 08540

Abstract

A gas puff imaging diagnostic is used in the National Spherical Tokamak Experiment [M. Ono, *et al.*, Nucl. Fusion **40**, 557 (2000)] to study the edge turbulence and intermittency present during H-mode discharges. In the case of low power Ohmic H-modes the suppression of turbulence/blobs is maintained through the duration of the (short lived) H-modes. Similar quiescent edges are seen during the early stages of H-modes created with the use of neutral beam injection. Nevertheless, as time progresses following the L-H transition, turbulence and blobs re-appear although at a lower level than that typically seen during L-mode confinement. It is also seen that the time-averaged SOL emission profile broadens, as the power loss across the separatrix increases. These broad profiles are characterized by a large level of fluctuations and intermittent events.

JNM Keywords: P0600 (plasma properties)

PSI-19 Keywords: edge plasma, intermittent transport, fluctuations and turbulence, NSTX, cross-field transport

PACS: 52.55.Fa, 52.35.Ra, 52.70.Kz

* Corresponding author: Ricardo Maqueda
Princeton Plasma Physics Laboratory
P.O. Box 451
Princeton, NJ 08543, USA
rmaqueda@pppl.gov

1. Introduction

Short time-scale intermittent events are routinely seen in the outboard scrape-off layer (SOL) of magnetically confined experiments. These coherent structures, most commonly named "blobs" [1-2], but also known as intermittent plasma objects [3], avaloids [4] or just inter-ELM filaments [5-8] can contribute up to 50% of the cross-field transport [3]. The origin of these intermittent events has been linked to edge turbulence [9] and, in a low pressure toroidal devices, they have been seen to originate from interchange modes [10]. In toroidally confined experiments the edge turbulence and intermittent events change in character as the plasma accesses the high confinement mode regime (H-mode) [11]. While in the DIII-D tokamak these changes present themselves as a reduction in the density and temperature within the ejected filaments [12], in the Alcator C-Mod device it has been recently seen that the turbulence present just inside the saparatrix is modified with the electron diamagnetic drifting branch of the power spectra having a relatively smaller amplitude during H-mode [13]. Nevertheless, the SOL intermittency in C-Mod does not normally change across the transition from low confinement mode (L-mode) to H-mode [14].

In this paper we present results from the National Spherical Torus Experiment (NSTX) [15]. In this experiment both the turbulence power and frequency of intermittent blobs are reduced in H-mode compared to L-mode. Although sheared flows, and perhaps zonal flows, are good candidates for causing the L vs. H differences observed in NSTX and other toroidal devices, little is known about the generation of these SOL blobs during H-mode confinement. This paper presents data from NSTX obtained with the Gas Puff Imaging (GPI) diagnostic [2, 16], showing a varied level of turbulence and intermittency during discharges that have accessed

H-mode confinement. This ranges from quiescent H-modes obtained during Ohmic (no auxiliary heating) discharges to highly active H-modes with high power neutral beam injection.

2. Experimental setup

The measurements described in this paper were obtained in the National Spherical Torus Experiment (NSTX) [15]. This experiment is a low aspect ratio tokamak with a major radius R = 0.86 m and a minor radius a = 0.67 m. Discharges with plasma current I_p = 0.8-1.2 MA and toroidal field on axis B_t = 0.45-0.50 T were used with auxiliary heating in the form of neutral beam injection (NBI) raging from 0 MW (i.e., only Ohmic heating) to 7 MW. Although both double null and single null X-point configurations as well as different elongations and triangularities were used, the characteristics of the edge turbulence and intermittency are not affected by these variations, at least to the extent of the results shown in this paper which are mainly due to changes in heating power. Plasmas in high confinement mode (H-mode) were used and although edge localized modes (ELMs) were present on some of these discharges, inter-ELM periods were used for the work presented here.

The main diagnostic used in the work presented in this paper was high frame rate imaging of the D_α edge emission. The cameras used, either a Phantom 7.1 or a Phantom 7.3, captured ~120000 frames/s yielding inter-frame times of 7 μs or 8.25 μs. The frame exposures used were 3-6 μs. The imaging system viewed a tangential, ~25 cm poloidal section of the edge just above the outer midplane of the plasma (Fig. 1). The pitch angle of the magnetic field in the viewing region of this tangential edge camera was selected so that the visible light emission was viewed along the direction of the local magnetic field line. In this way, "end-on" images of the field-aligned edge structure and filaments were obtained. In addition, a non-perturbing deuterium gas puff (~10 Torr l/s) was added in the field of view to further localize the emitting

region to a ~20 cm length along the line of sight and also increase the contrast and brightness of the D_α line emission which was selected with a narrowband interference filter. Degas 2 simulation of the D_α emission in this diagnostic setup indicates that the spatial structure of the emitting neutral cloud captured in the camera images reflects the structure of the plasma, despite a non-linear dependence of the emission on the electron density and temperature of this plasma [17]. Further details of this gas puff imaging (GPI) diagnostic, as well as of the non-perturbing condition of the gas puff itself, can be seen in Refs. [2] and [16].

3. Imaging results

The level of turbulence in the edge and the intermittent activity in the SOL is reduced when the plasmas in NSTX access H-mode confinement, as described in Ref. [2]. While in H-mode different levels of turbulence and intermittency are observed. Nevertheless, with the exception of the secondary filaments observed during ELMs [18], the H-mode edge/SOL activity is lower than that observed during L-mode. Examples from 4 different discharges are shown in Fig. 2. During Ohmic H-modes (Fig. 2(a)) the plasma edge remains quiescent with a very low level of turbulence and essentially no blobs being created. Similar results are obtained during the early stages of neutral beam heated H-modes (Fig. 2(b)), although turbulence and blobs generally re-appear later in time after the L-H transition. The time when the transition takes place (t_{L-H}) is indicated on top of each of the image sequences in Fig. 2. Two examples of turbulent/blobby sequences are shown in Figs. 2(c) and 2(d) obtained late after the transition. The blobs generated can propagate radially reaching the shadow of the antenna limiter. In the case of Ohmic H-modes, the current experimental database has only short H-mode phases (<30 ms) and consequently it is not known if turbulence and blobs would reappear if the H-mode could be extended longer.

Some of the statistical properties averaged over 20 ms of the D_α emission seen in the discharges shown in Fig. 2 are presented in Fig. 3. In Fig. 3(a) it is seen that the emission profiles late after the L-H transition are broader than the early ones with a long tail developing into the SOL. Also, the early profile for the NBI heated discharge being narrower than the early Ohmic profile. The RMS fluctuation level and skewness (asymmetry of the probability distribution function) profiles obtained from images late after the transition are also larger than those from the Ohmic H-mode case, both near the separatrix and in the SOL. In the case of the NBI heated, early sequence data the skewness near the separatrix remains low (near Gaussian skewness, i.e., ~0) while the fluctuation level throughout the profile and skewness in the SOL are high. This is may be due to n=3 TAE MHD modes [19] affecting the edge and sporadically triggering blobs that propagate into an otherwise low intensity D_α profile creating a large RMS and skewness region in the SOL.

In Fig. 4 the statistical properties of the D_α emission in the SOL, as measured 5 cm outside the peak of this emission, are related to the power loss across the separatrix:

$$P_{loss} = P_\Omega + P_{NBI} - P_{rad} - dW/dt$$

where P_Ω and P_{NBI} are the Ohmic and NBI heating powers respectively, P_{rad} is the radiated power and W is the stored energy. Due to the uncertainty in the separatrix position this corresponds to 3-5 cm into the SOL. In Fig. 4(a) the near-SOL D_α emission is normalized by the total emission seen in the profile, yielding a crude indication of the profile width. It is then seen that this width increases with P_{loss}, in agreement with the shown in Fig. 3(a). The database used for these plots contains discharges with different magnetic configurations (i.e., null bias, elongation, triangularity, etc) and different densities. The scatter plots in Figs 4(b) and 4(c) show that both the RMS fluctuation level and skewness remain high indicating the presence of intense

($\delta I/I \sim 100$-150%) fluctuations with intermittent characteristics (skewness > 2.0). The only exception to this trend is the Ohmic H-mode shots where the SOL fluctuation level is ~35%, although in/out movement of profile in the 20 ms time-scale used for the averaging and other diagnostic limitations contribute to this net fluctuation level beyond that strictly from intermittent events. The main contribution to the scaling seen in Fig. 4(a) is the frequency at which blobs are being generated (like in Fig. 2), also scaling well with P_{loss}, and not the characteristics of these intermittent events. We point out that in NSTX this frequency is also a notable difference observed between H-modes and L-modes.

4. Summary and conclusions

Measurements in the NSTX experiment using the gas puff imaging diagnostic have shown that the edge turbulence and SOL blobs are reduced during H-modes compared to L-mode. In the case of low power Ohmic H-modes the suppression of turbulence/blobs is maintained through the duration of the (short lived) H-modes. Similar results are obtained during the early stages of H-modes created with auxiliary NBI power, with suppression of edge/SOL activity. As time progresses following the L-H transition, turbulence and blobs re-appear although at a lower level than that typically seen during L-mode confinement (or soon after an ELM crash). It is also seen (Figs. 3-4) that the time-averaged SOL emission profile broadens, as the power loss increases. These broad profiles are characterized by a large level of fluctuations and intermittent events.

It has been proposed, and numerical models confirm, that the presence of sheared flows can be responsible for the suppression of turbulence and subsequent creation of intermittent blobs that then propagate radially across the SOL [9]. This appears to be consistent with the measurements, like those shown in Figs. 2(a) and 2(b). The question then arises regarding the

trigger mechanism for the reappearance of fluctuations and blob creation at later times after the L-H transition. One possible candidate for this trigger are MHD modes, as in the discharge shown in Fig. 2(b) one example where short bursts of MHD activity lead to few blobs being created. Nevertheless, at higher powers, like the discharges in Figs. 2(c) and 2(d) no MHD is present, yet edge fluctuations and blob creation are seen some time after the L-H transition. The mechanism responsible for the creation of blobs, including the role of MHD modes, is being investigated and it will be the subject of a subsequent publication.

We should point out that even though the increase in SOL emission width is clear from Fig. 4(a) as more power is lost across the separatrix, the results shown here do not indicate a causal relationship between the fluctuations and intermittency observed (Figs. 4(b) and 4(c)) with this increasing width. Experiments are being planned [20], as well as close collaboration with modelling efforts [21], to gather further information regarding the SOL width and the relative importance of turbulence and blobs in determining this width. Results from these planned experiments and analysis will be presented in a subsequent paper.

Acknowledgments

The EFIT equilibrium reconstructions were provided by S. A. Sabbagh (Columbia University) and mode identification was performed by E. D. Fredrickson (PPPL). The use of the LRDFIT equilibrium reconstruction code developed by J. Menard (PPPL) is also acknowledged.

Work supported by US DOE under grants DE-FG02-04ER54767 and DE-AC-09CH11466.

References

[1] J.L. Terry et al., Phys. Plasmas **10** (2003) 1739.

[2] S.J. Zweben et al., Nucl. Fusion **44** (2004) 134.

[3] J.A. Boedo et al., Phys. Plasmas **8** (2001) 4826.

[4] G.Y. Antar , G. Counsell, Y. Yu., B. LaBombard and P. Devynck, Phys. Plasmas **10** (2003) 419.

[5] N. Ben Ayed, A. Kirk, B. Dudson, S. Tallents , R.G.L. Vann, H. R. Wilson and the MAST team, Plasma Phys. Control. Fusion **51** (2009) 035016.

[6] B. Kurzan, C. Fuchs, A. Scarabosio, B.D. Scott and ASDEX Upgrade team, Plasma Phys. Control. Fusion **51** (2009) 065009.

[7] C. Silva, B. Gonçalves, C. Hidalgo, M.A. Pedrosa, W. Fundamenski, M. Stamp, R.A. Pitts and JET-EFDA contributors, J. Nucl. Mater. **390-391** (2009) 355.

[8] H. Tanaka, N. Ohno, N. Asakura, Y. Tsuji, H. Kawashima, S. Takamura, Y. Uesugi and the JT-60U team, Nucl. Fusion **49** (2009) 065017.

[9] D.A. Russell, J.R. Myra and D.A. D'Ippolito, Phys. Plasmas **16** (2009) 122304.

[10] I. Furno et al., Phys. Rev. Lett. **100** (2008) 055004.

[11] ASDEX Team, Nucl. Fusion **29** (1989) 1959.

[12] J.A. Boedo et al., Phys. Plasmas **10** (2003) 1670.

[13] I. Cziegler, J.L. Terry, J.W. Hughes and B. LaBombard, Phys. Plasmas **17** (2010) 056120.

[14] S.J. Zweben et al., Phys. Plasmas **9** (2002) 1981.

[15] M. Ono et al., Nucl. Fusion **40** (2000) 557.

[16] R.J. Maqueda et al., Rev. Sci. Instrum. **74** (2003) 2020.

[17] D.P. Stotler, B. LaBombard, J.L. Terry and S.J. Zweben, J. Nucl. Mater. **313-316** (2003) 1066.

[18] R.J. Maqueda, R. Maingi, J.-W. Ahn and the NSTX Team, J. Nucl. Mater. **390-391** (2009) 843.

[19] E.D. Fredrickson, et al., Phys. Plasmas **13** (2006) 056109.

[20] R. Maingi et al., this issue (Proceedings 19th PSI Conference, 2010)..

[21] J.R. Myra et al., this issue (Proceedings 19th PSI Conference, 2010).

Figure captions

Fig. 1. Schematic arrangement of the GPI diagnostic. The deuterium gas puff is introduced through a 30 cm-long tube with small (1 mm) perforations on its plasma facing side. The D_α emitting gas cloud is viewed along the direction of the local magnetic field. Edge filaments, parallel to this field, are then imaged as blobs.

Fig. 2. Different levels of activity are observed during H-mode with the GPI diagnostic. Each box in these image sequences shows a 24x24 cm portion of the edge just above the outer midplane. The inter-frame time is 8.25 μs for sequence (a) and 7.0 μs for sequences (b)-(d). The yellow solid line indicates the separatrix position as determined by LRDFIT equilibrium reconstructions. The dotted line represents the shadow of the RF antenna limiter. (Shot numbers: (a) 115514, (b) 135043, (c) 135490, (d) 135494)

Fig. 3. Statistical profiles averaged over 20 ms: (a) D_α profile, (b) root-mean-square (RMS) fluctuation level, (c) skewness of the distribution function. The separatrix position, uncertain to ±1 cm, is indicated with a gray region.

Fig. 4. Characteristics of the SOL emission as a function of the power loss across the separatrix. The SOL D_α emission is characterized in a ~1 cm band located 5 cm outboard from the peak of this emission, or 3-5 cm outside the separatrix.

Figure

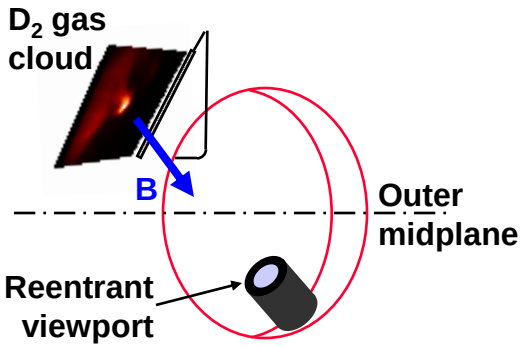

Figure

(a) Ohmic H-mode, 210.01 to 210.15 ms (t_{L-H}~193.5 ms)

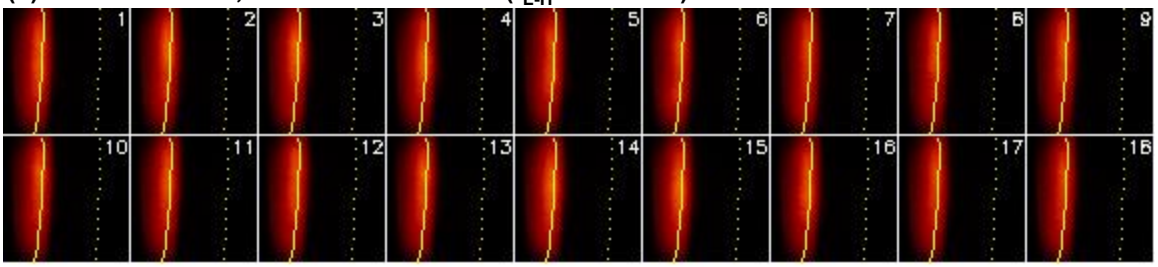

(b) 2.6 MW NBI early H-mode phase, 260.68 to 260.80 ms (t_{L-H}~249.6 ms)

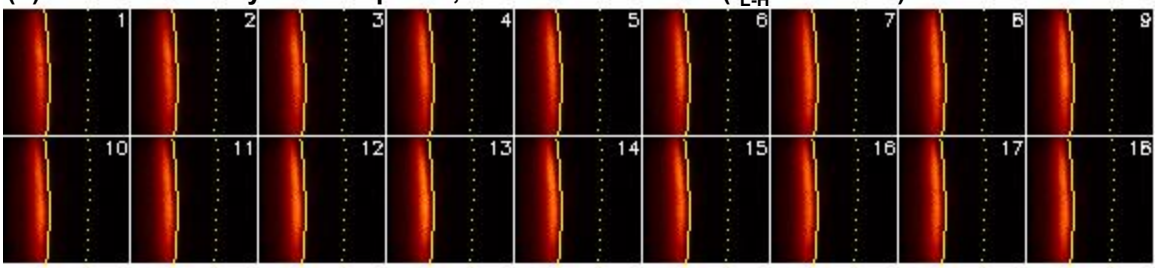

(c) 3.9 MW NBI late H-mode phase, 429.42 to 429.55 ms (t_{L-H}~156.1 ms)

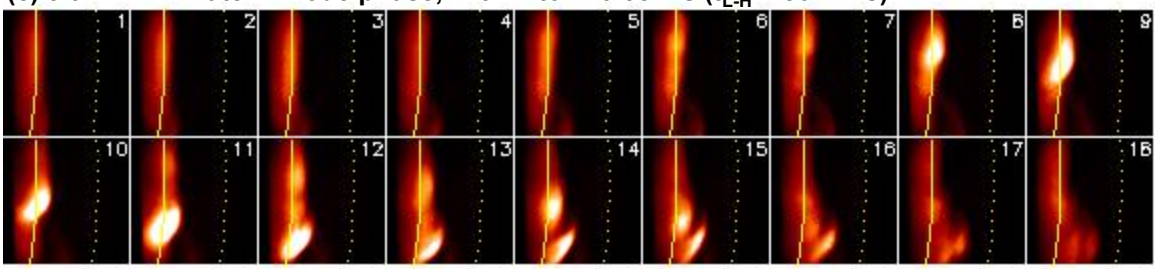

(d) 3.9 MW NBI late H-mode phase, 429.80 to 429.93 ms (t_{L-H}~194.0 ms)

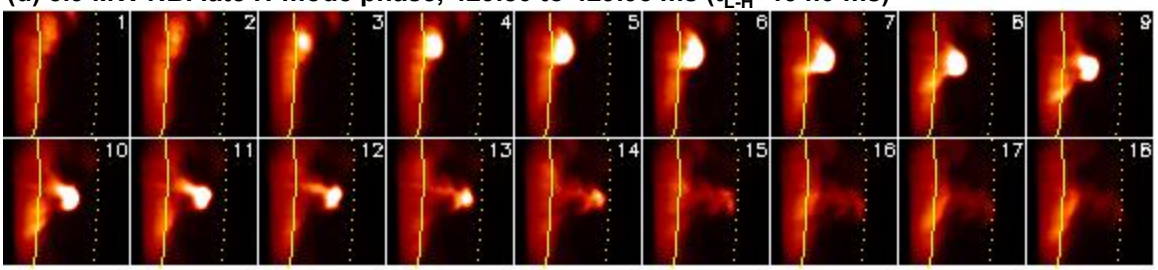

Figure

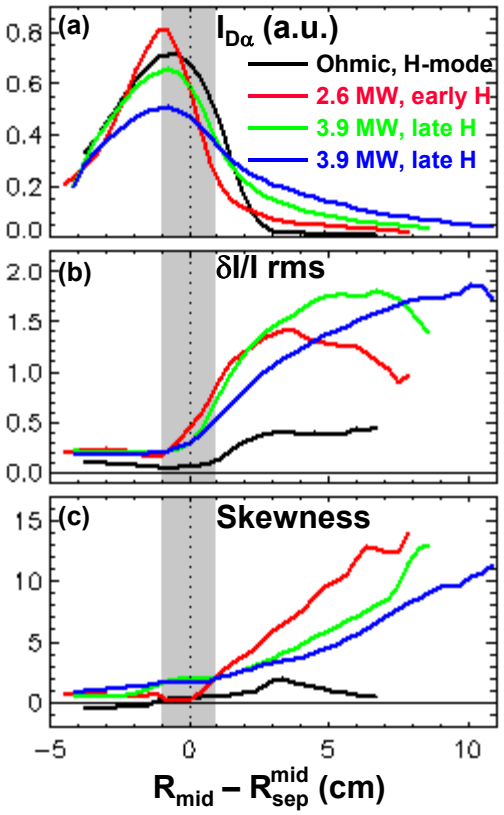
(a)
$I_{D\alpha}$ (a.u.)
Ohmic, H-mode
2.6 MW, early H
3.9 MW, late H
3.9 MW, late H
0.8
0.6
0.4
0.2
0.0
(b)
δI/I rms
2.0
1.5
1.0
0.5
0.0
(c)
Skewness
15
10
5
0
−5
0
5
10
$R_{mid} - R_{sep}^{mid}$ (cm)

Figure

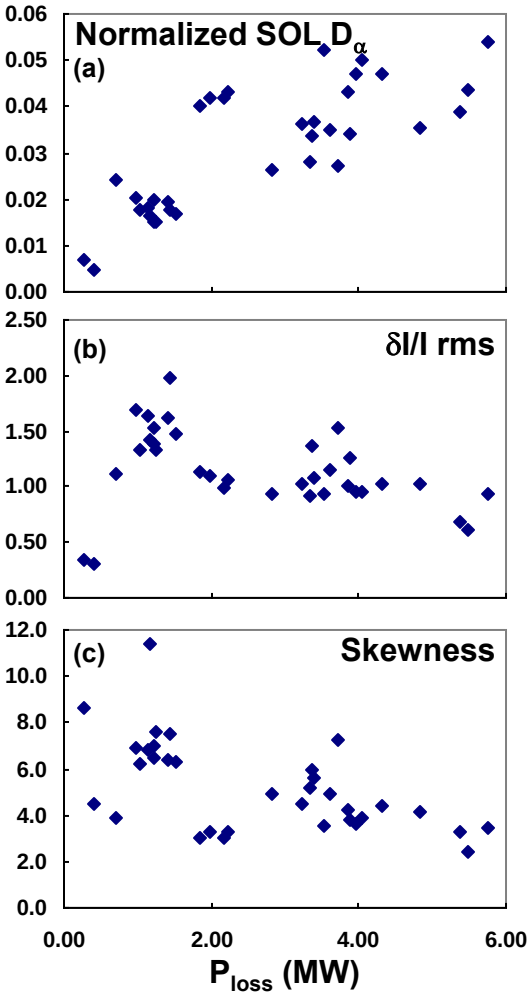
Normalized SOL D_α
(a)
0.06
0.05
0.04
0.03
0.02
0.01
0.00
(b)
δI/I rms
2.50
2.00
1.50
1.00
0.50
0.00
(c)
Skewness
12.0
10.0
8.0
6.0
4.0
2.0
0.0
0.00
2.00
4.00
6.00
P_{loss} (MW)